ChemPubSoc Europe

DOI: 10.1002/cbic.201402095

Crystal Structures of Acyl Carrier Protein in Complex with Two Catalytic Partners Show a Dynamic Role in Cellular Metabolism

Sean A. Newmister[b] and David H. Sherman*[a]

Acyl carrier proteins (ACPs) are small, highly conserved proteins that play an essential role in the transport and delivery of hydrocarbon substrates in numerous biosynthetic systems across all domains of life. Notably, ACPs participate in the biosynthesis of fatty acids, polyketides, and lipopolysaccharides in which starting materials and intermediates are transported sequentially among biosynthetic enzymes by ACP through a thioester linkage to a covalently attached phosphopantetheine group. ACPs can function as part of a larger polypeptide (type I) with additional catalytic domains, including modular polyketide synthase (PKS) and eukaryotic fatty acid synthase (FASI), or as a discrete polypeptide (type II) that interacts with various catalytic partners (e.g., bacterial FASII and the lipid A pathway).

The type II *Escherichia coli* ACP has 21 known catalytic binding partners, many of which are involved in the biosynthesis of fatty acids and lipid A. These pathways are essential for viability in *E. coli* and have attracted considerable interest due to their fundamental role in primary metabolism as well as their demonstrated potential as therapeutic targets. A central question therein relates to the remarkable selectivity with which acyl-ACPs are able to associate with the appropriate catalytic partner in a substrate-dependent manner. Although structural elucidation could offer valuable insight into specific ACP–enzyme interactions, detailed characterization is scarce owing to the weak and transient nature of ACP–enzyme interactions and to the conformational flexibility of ACP, though several NMR and X-ray crystal structures of stand-alone ACPs have been reported. In these structures, ACP is shown to form a helical bundle in which the thioester-linked acyl chain is sequestered from the solvent in an internal hydrophobic cavity. This cavity is dynamic and can accommodate substrates of various size and composition. Structures of ACP in complex with binding partners as well as biochemical experiments have provided evidence for the role of acidic helices II and III as key recognition elements in ACP–partner interactions, thereby refining significantly our understanding of these associations.[1] Recently in *Nature*, two high-resolution crystal structures of transient acyl–ACP partner complexes that capture the carrier-protein-mediated delivery of substrate were reported. These structures provide the first crystallographic snapshot of substrate delivery by ACP, as well as several clues about the role of ACP dynamics during catalysis.

Burkart, Tsai, and co-workers reported the structure of a crosslinked *E. coli* FabA–ACP complex that was generated through the use of a sulfonyl-alkyne mechanism-based probe (Figure 1 A).[2] FabA is a dehydratase that acts on 3-hydroxydecanoyl-ACPs, thus providing the first high-resolution structure of a FASII enzyme in which the ACP-mediated substrate delivery can be visualized.[3] In this structure, two ACP molecules are associated with the FabA homodimer (Figure 1 B). Surprisingly, the ACPs are conformationally distinct with 503 and 539 Å^2 buried surface area between the two ACP–FabA interfaces. These ACPs are free from close crystal contacts that could introduce aberrant association with FabA. Thus the authors surmised that the dual ACP binding modes with FabA homodimer represent a fully docked ACP as well as ACP in transition.

Key residue contacts implicated by the crystal structure were verified by ^{1}H/^{15}N HSQC NMR spectroscopy in which chemical shift perturbations with FabA and butyl-ACP were observed that aligned with those of the crosslinked complex. These spectra provide a dynamic view of the key residues involved in complex formation and substrate delivery, with the most pronounced shifts occurring on the ACP at helix II and helix III that contact a "positive patch" on FabA (Figure 2 A) and within the hydrophobic substrate binding pocket, which collapsed to extrude acyl substrate. These data corroborate an in vivo analysis in which many of the same residues were shown to be essential for ACP function,[4] and also support the "switchblade" mechanism proposed by Ban based on the *Saccharomyces cerevisiae* FASI structure.[5] In addition to key protein–protein interactions, these data revealed conformational changes within the ACP that likely drive complex formation and dissociation. These rearrangements are largely centered about the acidic residues on ACP helices II and III and are likely facilitated by motion at the helix II–III loop, as confirmed by molecular dynamics simulations (Figure 2 C).

In a second study relating to ACP dynamics, Pemble and coworkers reported the structure of LpxD in complexes that represent three states of its catalytic cycle: acyl-ACP, ACP-hydrolyzed substrate, holo-ACP (Figure 1 D).[6] LpxD catalyzes the transfer of (*R*)-3-hydroxymyristoyl (β-OH-C_{14}) acyl chains to

[a] *Prof. D. H. Sherman*
Life Sciences Institute and Departments of Medicinal Chemistry, Chemistry, and Microbiology & Immunology, University of Michigan
210 Washtenaw Avenue, Ann Arbor, MI 48109 (USA)
E-mail: davidhs@umich.edu

[b] *Dr. S. A. Newmister*
Life Sciences Institute, University of Michigan
210 Washtenaw Avenue, Ann Arbor, MI 48109 (USA)

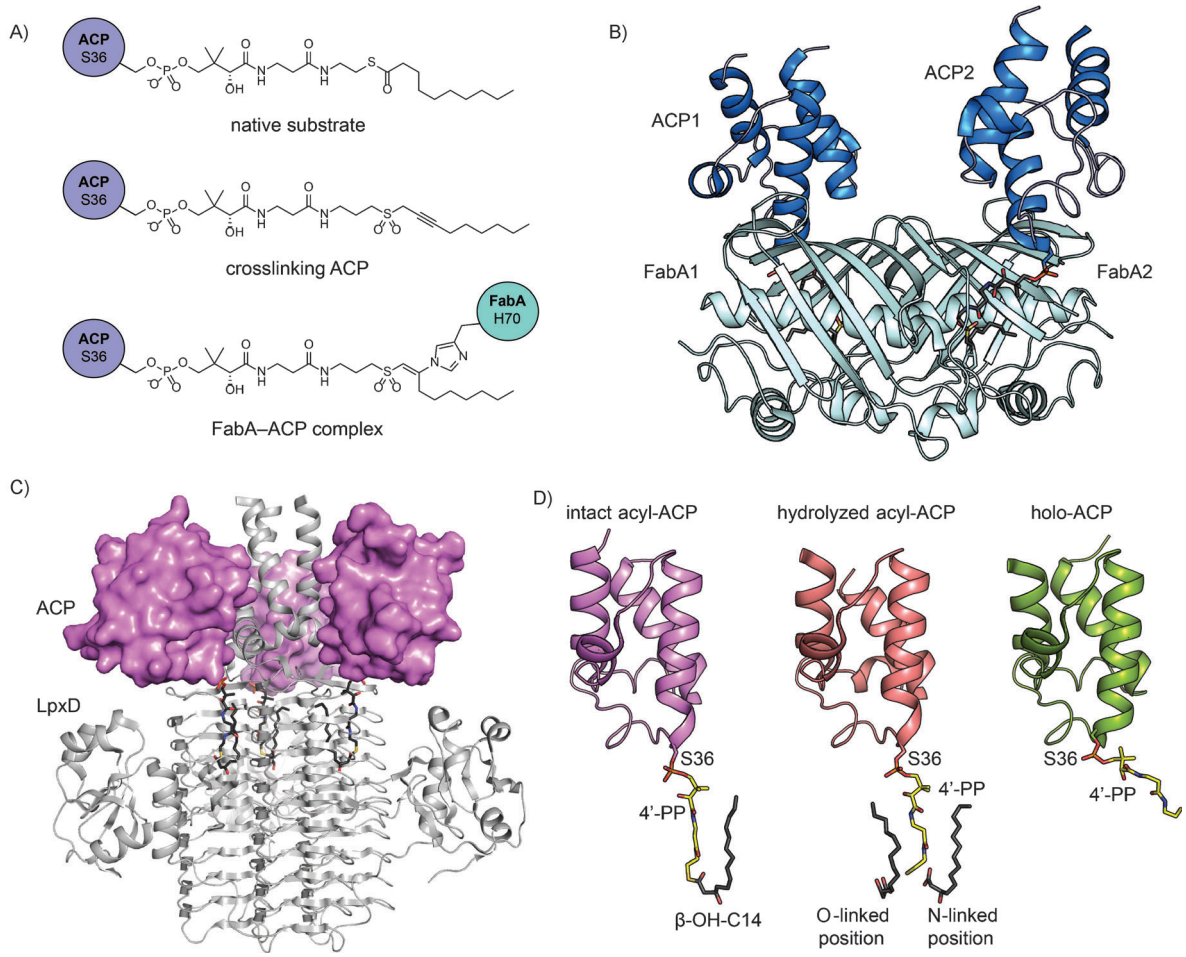

Figure 1. Structures of FabA–ACP and LpxD–ACP complexes. A) The native 3-hydroxydecanoyl-ACP substrate for FabA (top) compared to the sulfonyl-3-alkynyl mechanism-based probe (middle) that was used to generate a uniformly crosslinked FabA–ACP construct (bottom) for crystallization. B) Structure of the crosslinked FabA–ACP homodimer; ACP1 and ACP2 (blue) differ markedly in their association with FabA (cyan). C) Cartoon representation of the LpxD homotrimer (light gray) in complex with three acyl-ACP molecules (surface, magenta). D) Structures of LpxD in complex with various ACP forms visualize three key steps (intact acyl-ACP in magenta, hydrolyzed acyl-ACP in salmon, and holo-ACP in green) along the LpxD reaction coordinate. The figure was generated by using PyMOL.

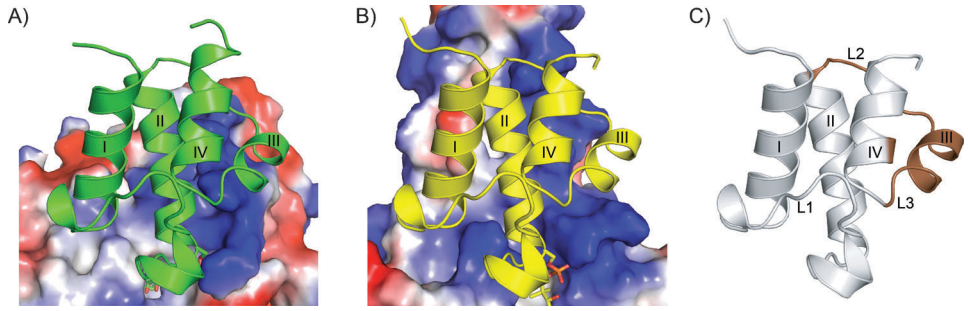

Figure 2. Association of ACP with two catalytic partners. A) ACP (green) interacts with the "positive patch" of FabA (electrostatic surface representation). B) In the LpxD structure, ACP (yellow) associates with the basic ACP recognition domain on LpxD (electrostatic surface representation). C) Key dynamic regions involved in complex dissociation are highlighted in brown. These residues are clustered about loop 2 and helix 3 and were identified by HSQC NMR and molecular dynamics,[2c] as well as alignment of the LpxD–acyl-ACP and LpxD–holo-ACP structures.[6]

UDP-acyl-GlcN to generate UDP-diacyl-GlcN in lipid A biosynthesis through an ordered sequential kinetic mechanism.[7] LpxD is a homotrimer in which three active sites are formed at the interface between adjacent subunits (Figure 1C).[8] This array of structures uncovers several key interactions between carrier protein, 4′-phosphopantetheine, acyl substrate, and LpxD, again providing unprecedented insights into both the association and dissociation of ACP and its catalytic partners.

With regard to complex formation, extensive electrostatic interactions are observed between carrier protein and LpxD, which is highly similar to that of FabA (Figure 2B). Moreover, numerous LpxD contacts line the phosphopantetheine arm and acyl substrate in the acyl-ACP structure. These new insights reveal the molecular basis for the selectivity of LpxD for C_{14} acyl chains based on the close packing of Met290 against the terminal carbon atoms of β-OH-C14, and through an extensive

hydrogen bond network about the β-hydroxy group. In the structure with hydrolyzed substrate, a second acyl chain reveals the likely binding site for the O-linked acyl chain of the UDP-acyl-GlcN substrate. Finally, in the structure with holo-ACP, the last complex in the reaction coordinate, the ACP–LpxD complex is destabilized, as indicated by high *B*-factors and the weak electron density of carrier protein. Furthermore contact between the 4′-phosphopantetheine thiol and Met290 in the holo-ACP structure uncovered an unexpected role of the ACP prosthetic group in complex dissociation. The movement of 4′-phosphopantetheine opens the previously blocked reaction chamber enabling release of the UDP-diacyl-GlcN product and triggering complex dissociation.

Comparison of these three structures enabled the authors to track the movements of ACP at three key points along the LpxD reaction coordinate. The greatest displacement was observed both in the helix II–III loop and in helix III of ACP where several electrostatic contacts with LpxD were broken in the hydrolyzed and holo-ACP complexes (Figure 2C). These structural shifts are strikingly similar to those reported by Burkart, Tsai, and co-workers, and point to the general role that these regions play in ACP-based associations, and presumably to dissociation of the complex as well.

The ACP complex structures of FabA and LpxD clarify our understanding of the dynamic nature of ACP with respect to its interactions with partner proteins. In both cases, the authors directly observed extensive contacts with 4′-phosphopantetheine-linked substrate and key electrostatic interactions with the ACP. Both crystallographic and computational evidence points to conformational changes in ACP that drive substrate delivery and complex dissociation. Together these studies provide a remarkable basis for understanding in molecular detail the dynamic role of ACP, which might ultimately be extended to the numerous carrier-protein-dependent pathways in primary and secondary metabolism.

Acknowledgement

The authors gratefully acknowledge support from NIH grant GM076477 and the Hans W. Vahlteich Professorship (D.H.S.).

Keywords: acyl carrier proteins · biosynthesis · fatty acids · lipid A

[1] J. Crosby, M. P. Crump, *Nat. Prod. Rep.* **2012**, *29*, 1111 – 1137.
[2] a) F. Ishikawa, R. W. Haushalter, M. D. Burkart, *J. Am. Chem. Soc.* **2012**, *134*, 769 – 772; b) G. M. Helmkamp Jr., K. Bloch, *J. Biol. Chem.* **1969**, *244*, 6014 – 6022; c) C. Nguyen, R. W. Haushalter, D. J. Lee, P. R. Markwick, J. Bruegger, G. Caldara-Festin, K. Finzel, D. R. Jackson, F. Ishikawa, B. O'Dowd, J. A. McCammon, S. J. Opella, S. C. Tsai, M. D. Burkart, *Nature* **2014**, *505*, 427 – 431.
[3] L. R. Kass, K. Bloch, *Proc. Natl. Acad. Sci. USA* **1967**, *58*, 1168 – 1173.
[4] N. R. De Lay, J. E. Cronan, *J. Biol. Chem.* **2007**, *282*, 20319 – 20328.
[5] M. Leibundgut, S. Jenni, C. Frick, N. Ban, *Science* **2007**, *316*, 288 – 290.
[6] A. Masoudi, C. R. Raetz, P. Zhou, C. W. Pemble IV, *Nature* **2014**, *505*, 422 – 426.
[7] M. S. Anderson, C. R. Raetz, *J. Biol. Chem.* **1987**, *262*, 5159 – 5169.
[8] a) L. Buetow, T. K. Smith, A. Dawson, S. Fyffe, W. N. Hunter, *Proc. Natl. Acad. Sci. USA* **2007**, *104*, 4321 – 4326; b) C. M. Bartling, C. R. Raetz, *Biochemistry* **2009**, *48*, 8672 – 8683.

Received: March 13, 2014
Published online on April 25, 2014